

Combustion and Emissions of 2,5-Dimethylfuran in a Direct-Injection Spark-Ignition Engine

Shaohua Zhong,[†] Ritchie Daniel,[†] Hongming Xu,^{*,†} Jun Zhang,[†] Dale Turner,[†]
Mirosław L. Wyszynski,[†] and Paul Richards[‡]

[†]The University of Birmingham, Birmingham B15 2TT, United Kingdom, and [‡]Innospec, Incorporated, Cheshire CH65 4EY, United Kingdom

Received January 16, 2010. Revised Manuscript Received March 25, 2010

Biomass has the potential to become an important source of energy for future automotive fuels. Recent biological and chemical improvements to the conversion of biomass-derived carbohydrates have produced high yields of liquid 2,5-dimethylfuran (DMF). This discovery has made DMF a possible substitute for petroleum-based gasoline, because they share very similar physicochemical properties, which are superior to those of ethanol. In the present study, experiments have been carried out on a single-cylinder gasoline direct-injection (GDI) research engine to study the performance of DMF benchmarked against gasoline and what is considered to be the current biofuel leader, ethanol. Initial results are very promising for DMF as a new biofuel; not only is the combustion performance similar to commercial gasoline, but the regulated emissions are also comparable.

1. Introduction

Biofuels have a part to play in the supply of renewable energy. They can help reduce the contribution of the automotive industry to greenhouse gas emissions and help protect the environment. The use of renewable energy sources is likely to increase in the future with the development of new generation biofuels, which are much more efficient in terms of their carbon footprint while at the same time becoming easier to use in engines. Some of the key questions governing the success of such biofuels include the provenance of raw materials, their production methods, the distribution infrastructure, the raw material availability, their production costs, and most typically, their lifecycle carbon footprint.

Recently, significant progress in the technology of new biofuels has been made by bioscientists in the U.S.^{1,2} Using a new catalytic biomass–liquid process to catalyze the conversion of both fructose and, even more importantly, glucose into 5-hydroxymethylfurfural (HMF), an exceptionally high yield of 2,5-dimethylfuran (DMF, C₆H₈O, shown in Figure 1) has been demonstrated. Román-Leshkov et al. have developed a two-stage process to convert the biomass-derived sugar into DMF,¹ while Zhao et al. have studied the production of HMF from sugars.² Their focus was to efficiently convert glucose to fructose and, finally, to HMF using a metal chloride catalyst with ionic liquid solvents. More recently, Mascal et al.³ have converted cellulose to 5-(chloromethyl)furfural, which can be hydrogenized to DMF.

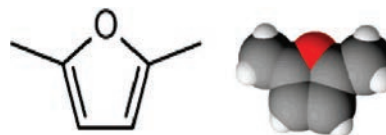


Figure 1. Molecular structure of DMF.

These findings have revitalized the potential of using DMF as an automotive energy carrier. As an alternative biofuel, DMF exhibits a number of attractive features. For instance, it has a relatively high volumetric energy density (31.5 MJ/L),⁴ which is comparable to that of gasoline (32.2 MJ/L) and almost 40% higher than that of ethanol (23 MJ/L). DMF is also believed to have a high research octane number (119),¹ which will allow for the use of high engine compression ratios for improved fuel economy. DMF is stable in storage and insoluble in water (see Table 2). Therefore, it will not become contaminated through water absorption from the atmosphere (in comparison to the high miscibility of ethanol). More attractively, DMF consumes only one-third of the energy in the evaporation stage of its production, in comparison to that required by fermentation for ethanol.¹ In fact, the catalytic strategy successfully developed for the production of DMF from building blocks of carbohydrates, cellulose (fructose or glucose), has made the large-scale and low-cost production of DMF possible.^{2,3} The implication of this breakthrough is significant, because DMF shares very similar physicochemical properties to gasoline, as previously discussed. However, its wide application as a main automotive fuel has been prevented by limited historical supply and commercial availability.

Despite the developments in the biomass conversion technology, which may have paved the way for the mass production of DMF as a new biofuel candidate, there are some

*To whom correspondence should be addressed. Telephone: 0044-121-4144153. Fax: 0044-121-4143958. E-mail: h.m.xu@bham.ac.uk.

(1) Román-Leshkov, Y.; Barrett, C. J.; Liu, Z. Y.; Dumesic, J. A. Production of dimethylfuran for liquid fuels from biomass-derived carbohydrates. *Nature* **2007**, *447*, 982–985.

(2) Zhao, H.; Holladay, J. E.; Brown, H.; Zhang, Z. C. Metal chlorides in ionic liquid solvents convert sugars to 5-hydroxymethylfurfural. *Science* **2007**, *316* (5831), 1597–1600.

(3) Mascal, M.; Nikitin, E. B. Direct, high-yield conversion of cellulose into biofuel. *Angew. Chem., Int. Ed.* **2008**, *47* (41), 7924–7926.

(4) Binder, J. B.; Raines, R. T. Simple chemical transformation of lignocellulosic biomass into furans for fuels and chemicals. *J. Am. Chem. Soc.* **2009**, *131*, 1979–1985.

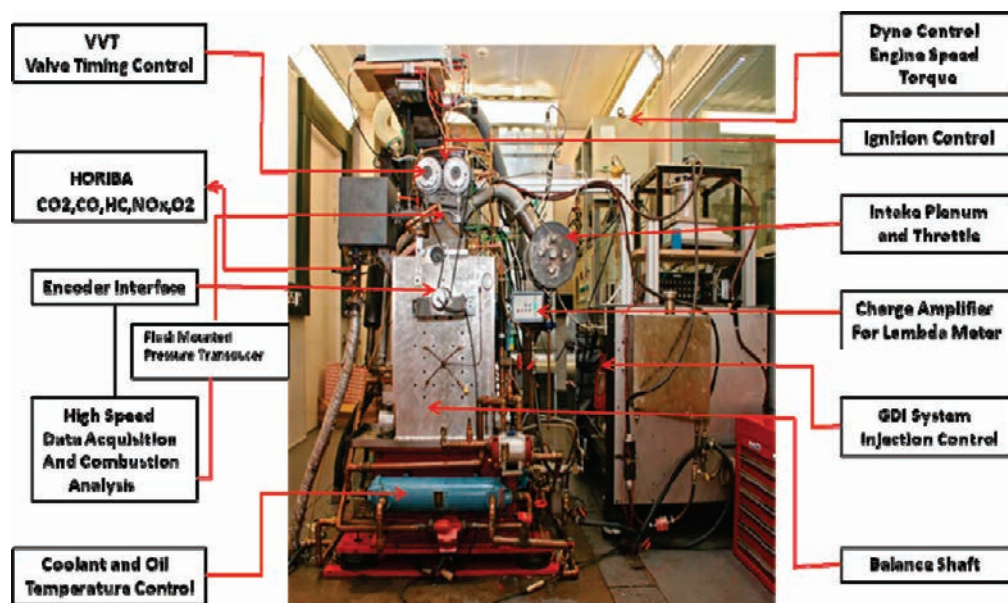


Figure 2. Test engine and experimental system.

Table 1. Engine Geometry and Valve Event Details

geometry details		valve timing details	
engine type	four stroke, four valve	intake valve lift (mm)	10.5
swept volume (cm ³)	565.6	intake valve duration	250° CAD
stroke (mm)	88.9	exhaust valve lift (mm)	9.3
bore (mm)	90	exhaust valve duration	250° CAD
connecting rod length (mm)	160	IVO	16° BTDC
piston offset (mm)	0.6	EVC	36° ATDC
compression ratio	11.5	spark timing	24°, 34°, and 44° BTDC
fueling type	spray-guided DI	fuel injection pressure and timing	150 bar with SOI at 280° BTDC

outstanding issues that remain unresolved before it can be commercialized. Little is currently known about the combustion and emission characteristics of DMF,^{5,6} especially the speciation of the unregulated emissions and their toxicities. However, reports are beginning to emerge on the laminar flame characteristics of DMF combustion.^{5,6} If DMF can be accepted as an alternative transportation fuel, extensive engine performance and emissions research is required.¹

This paper is believed to be the world's first investigation on the use of DMF as a biofuel in a single-cylinder, spark-ignition, GDI (gasoline direct-injection) engine. The research is focused on the characteristics of combustion and conventional emissions of DMF, with comparisons made to ethanol and gasoline. In the following sections, a brief description of the experimental setup and procedure is given and then the results of various test runs are presented. Finally, major conclusions from this work are outlined in section 4.

2. Experimental Section

2.1. Test Engine. The test engine used for this study (shown in Figure 2) is a single-cylinder, four-stroke, spark-ignition, direct-injection (DI) engine, which has been described in

previous publications.⁷ It has benefited from several recent upgrades,⁷ adopting the Jaguar V8 AJ133 DI combustion system with dual variable valve timing control for both the intake and exhaust valves. A summary of the engine geometry is given below in Table 1.

The research engine was fitted with a DI fuel system. In the present study, the fuel was delivered by a free piston accumulator that was pressurized to 150 bar using bottled nitrogen (oxygen free). The fuel injection pressure was monitored by a fuel-line pressure meter. The system was fully purged using nitrogen when changing fuels to minimize contamination. The inlet system includes an air filter, a rotary gas volumetric flow meter, and a manually adjusted throttle. In this study, no external exhaust gas recirculation (EGR) was applied.

The cylinder pressure was measured with a Kistler-type 6125A pressure transducer fitted flush with the wall of the combustion chamber and connected via a Kistler 5011 charge amplifier to a National Instruments data acquisition card. Samples were taken at 0.5° crank angle degree (CAD) intervals for 100 consecutive cycles. The crankshaft position was measured using a digital shaft encoder. Coolant and oil temperatures were controlled at 85 and 95 °C (±3 °C), respectively, via a proportional integral differential (PID) controller. Various temperatures, e.g., air inlet and exhaust port temperatures, were measured with K-type thermocouples.

(5) Wu, X.; Huang, Z.; Yuan, T.; Zhang, K.; Wei, L. Identification of combustion intermediates in a low-pressure premixed laminar 2,5-dimethylfuran–oxygen–argon flame with tunable synchrotron photoionization. *Combust. Flame* **2009**, *156* (7), 1365–1376.

(6) Wu, X.; Huang, Z.; Yuan, T.; Jin, C.; Wang, X.; Zheng, B.; Zhang, Y.; Wei, L. Measurements of laminar burning velocities and Markstein lengths of 2,5-dimethylfuran–air–diluent premixed flames. *Energy Fuels* **2009**, *23* (9), 4355–4362.

(7) Turner, D.; Tian, G.; Xu, H. M.; Wyszynski, M. L.; Theodoridis, E. An experimental study of diesel combustion in a direct injection engine. SAE Tech. Pap. 2009-01-1101, 2009.

Table 2. Comparison of Fuel Properties

properties		DMF	ethanol	gasoline
molecular formula		C ₆ H ₈ O	C ₂ H ₆ O	C ₂ –C ₁₄
molecular mass	kg/kmol	96.13	46.07	100–105
density at 20 °C	kg/m ³	889.7	790.9	744.6
water solubility at 25 °C	mg/mL	insoluble, ≤1.47	highly soluble, ≥100	insoluble
gravimetric oxygen content	%	16.67	34.78	0
H/C ratio		1.33	3.00	1.865
O/C ratio		0.17	0.5	0
stoichiometric air/fuel ratio		10.72	8.95	14.56
gravimetric calorific value (LCV, liquid fuel)	MJ/kg	33.7	26.9	43.2
volumetric calorific value (LCV, liquid fuel)	MJ/L	30	21.3	32.2
research octane number (RON)		119	110	95.8
auto-ignition temperature	°C	285.85	423	257
latent heat of vaporization at 20 °C	kJ/mol	31.91	43.25	38.51

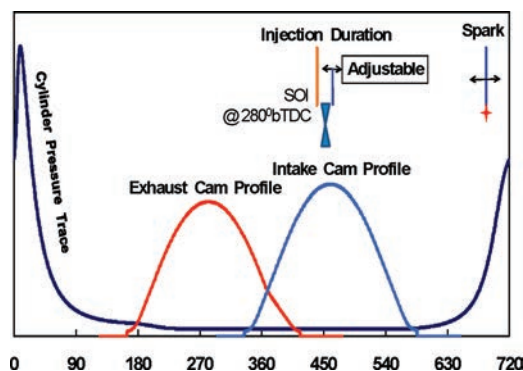


Figure 3. Valve, injection, and spark timing strategy.

The engine-operating parameters (injection, valve, spark timing, etc.) are set, as shown in Figure 3, using in-house software written in the LabVIEW programming environment. Similarly, high-speed data acquisition (crank angle resolved in-cylinder pressure) and low-speed data acquisition (time-resolved temperatures and gaseous emissions) were both achieved using LabVIEW-based in-house codes. Data analysis was conducted using an in-house developed MATLAB code. Data resulting from the analysis of consecutive engine cycles were calculated, including the peak cylinder pressure, indicated mean effective pressure (IMEP), coefficient of variation (COV) of IMEP, combustion duration, and the 10–90% burn points [10 and 90% mass fraction burned (MFB)].

The engine was coupled to an eddy direct current (DC) dynamometer to maintain a predetermined constant speed of 1500 revolutions per minute (rpm) (± 2 rpm) for this study, regardless of torque (motoring or firing conditions).

2.2. Gaseous Emission Measurement and Analysis. Gaseous emissions were measured by a HORIBA MEXA 7100DEGR gas analyzer, incorporating a heated line and prefilter. Gas samples were taken at 0.3 m downstream of the exhaust valve and transported via a heated line (maintained at 191 °C) to the gas analyzer. The air/fuel ratio was measured and monitored by an ETAS LA4 λ meter in conjunction with a Bosch LSU λ sensor, which uses fuel-specific curves to convert oxygen content and calculate excess air ratio (λ) values based on the carbon balance principle.

2.3. Particulate Sampling System. Particulate emissions were measured using a model 3936 scanning mobility particle sizer (SMPS) spectrometer manufactured by TSI Co., Inc. It comprises a 3080 electrostatic classifier, a 3775 condensation particle counter (CPC), and a 3081 differential mobility analyzer (DMA). Particulate samples were taken from the same position in the exhaust manifold as the gas sampling by

a dilutor. The SMPS was set to measure particles in the size range of 7.23–294.3 nm. The dilution ratio was set to 100:1.

2.4. Test Fuels and Experimental Procedure. The test fuels used in this study were 95 research octane number (RON) gasoline, bioethanol (both supplied by Shell Global Solutions U.K.), and DMF (99.8% purity from Shijiazhuang Lida Chemical Co., Ltd., China). Table 2 shows the properties of the three fuels used in this study.

All engine tests were conducted with ambient air inlet temperature (approximately 25 °C). Prior to data collection, the engine was started and warmed until the coolant and lubricating oil temperatures had reached 85 and 95 °C, respectively. After the warm-up phase, the engine was operated at a constant engine speed of 1500 rpm. All tests were carried out with an air/fuel ratio of 1.0. Comparisons of experimental data between the cases of DMF, gasoline, and ethanol were made under the same test conditions. The fuel injection pulse width and throttle area were varied to define the test conditions of the engine operation. As the load was varied, the spark timing, however, was held at 34° before top dead center (BTDC), which is the maximum brake torque (MBT) timing for 95 RON gasoline at 3.42 bar using this engine. The intention was to characterize the combustion performance of the three different fuels under the same engine-operating conditions. During the experiments, audible engine knocking became noticeable around 6 bar IMEP for both DMF and gasoline. These results were included until the knock became more obvious above 7.1 bar IMEP to show the combustion characteristics. Ethanol combustion, however, did not initiate knock at any load. This is investigated and explained later in the paper in section 3. A future paper will document the comparative performance of the three fuels under their respective optimized timing conditions. At each stable test condition (COV of IMEP <5%), the gaseous/particulate matter (PM) emissions and the in-cylinder pressure data were recorded to calculate the IMEP, combustion duration, combustion efficiency, etc.

3. Results and Discussion

3.1. Fuel Consumption. Figure 4a illustrates the comparison between the fuel rates in liters per hour at various engine load conditions using the three pure fuels. To provide the equivalent energy output of 1 L of gasoline, 1.512 L of ethanol and 1.073 L of DMF were required. Because each fuel has a different stoichiometric AFR (see Table 2), the throttle position was adjusted to maintain $\lambda = 1.0$ at the given load or IMEP. With increased throttle area, the mass flow through the manifold increases and the fuel quantity required to keep the air/fuel equivalence ratio at 1.0 also increases. Of the three fuels, ethanol has the lowest volumetric calorific value.

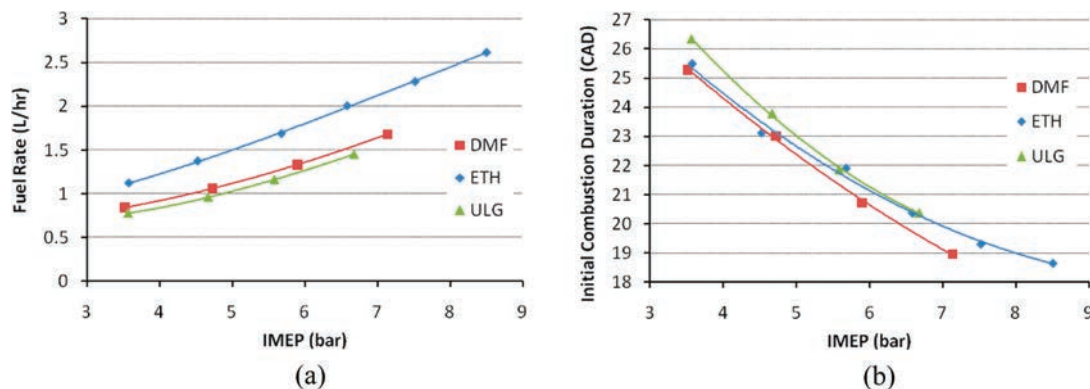


Figure 4. (a) Fuel flow rate (gasoline equivalent) and (b) initial combustion duration under different engine loads for DMF, ethanol, and gasoline at 1500 rpm and $\lambda = 1.0$.

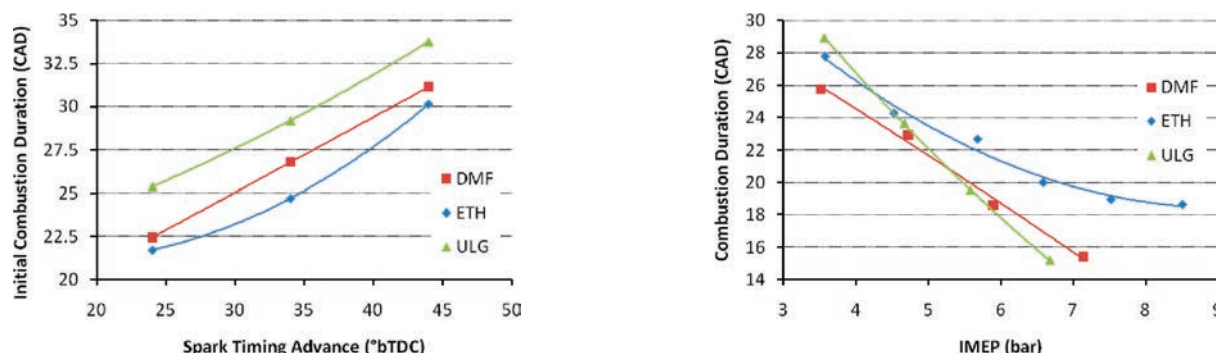


Figure 5. Initial combustion duration (ignition to 5% MFB) for DMF, ethanol, and gasoline under different spark timing values at 1500 rpm, IMEP = 3.0 bar, and $\lambda = 1.0$.

Therefore, to maintain the same engine load, more ethanol is required, which increases the fuel injection duration and, hence, the fuel flow rate, compared to gasoline and DMF. This relatively poor fuel economy is well-known. Published literature on ethanol/gasoline blends,^{8,9} for instance, have shown that when E20 is used (20 vol % of ethanol in gasoline), the fuel injection quantity required to maintain the engine power has to be increased.

Figure 4a highlights this fuel economy drawback when using ethanol. The fuel rate for ethanol is at least 33% more than that of gasoline throughout the entire load range. DMF, however, is very similar to gasoline, which is largely due to the similar gravimetric calorific values and relatively high density. As seen in Table 2, the volumetric calorific value of ethanol is 34% lower than that of gasoline, whereby DMF is only 7% lower.

3.2. Combustion Phasing. Figure 4b shows the initial combustion duration (the difference, in crank angle, between the spark timing and the 5% MFB point) for DMF, ethanol, and gasoline, under different values of IMEP for a constant ignition timing of 34° BTDC (MBT timing at 3.42 bar for gasoline). The trend in initial combustion phasing is similar for the three fuels as the IMEP increases. It can be seen that, at the lower values of IMEP, the initial combustion duration is longer and that, as expected, the initial combustion

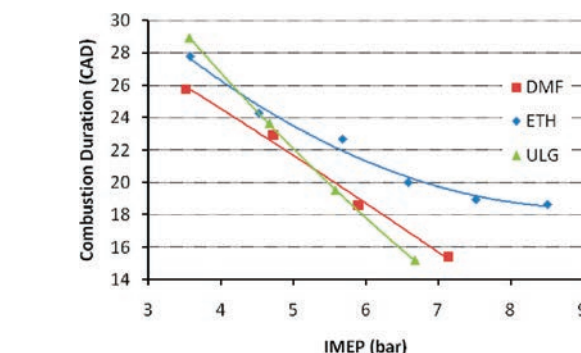


Figure 6. Combustion duration (10–90% MFB) for DMF, ethanol, and gasoline at 1500 rpm, $\lambda = 1.0$, and ignition at 34° BTDC.

duration gradually decreases with an increasing IMEP. Between the fuels, DMF exhibits a lower initial combustion duration compared to gasoline and ethanol for the range of IMEPs tested, which is magnified at higher engine loads (7.1 bar).

Despite this, it cannot be concluded here that DMF has better ignitability than ethanol and gasoline if the differences in the in-cylinder pressures and temperatures are considered for the test conditions. However, at the lower load condition of 3.0 bar IMEP and constant spark timing of 34° BTDC, it is ethanol that has the lowest initial combustion duration. This is shown in Figure 5, which is in-line with the trend observed in Figure 4b. In Figure 5, the spark timing has been varied between 24° and 44° BTDC at 3.0 bar IMEP. It is apparent that the initial combustion duration of DMF is smaller than that of gasoline but bigger than that of ethanol at this engine condition. The initial combustion duration increases for all three fuels when the spark timing is advanced because of the lower in-cylinder charge temperature and pressure at the point of ignition. In fact, it is ethanol that has the lowest in-cylinder gas temperature, shown later in Figure 9b, which suggests that it has the best ignitability because of the low initial combustion duration under these physical conditions.

Figure 6 compares the combustion durations of DMF, ethanol, and gasoline at a constant spark timing of 34° BTDC for the entire load range. The combustion duration is defined as the difference in crank angle position (in degrees) between the 10 and 90% MFB points. It can be seen that the combustion duration is different for the three fuels. Apart from 3.5 bar IMEP, the combustion duration when using ethanol is the highest for all of the loads tested.

(8) Sandquist, H.; Karlsson, M.; Denbratt, I. Influence of ethanol content in gasoline on speciated emissions from a direct injection stratified charge SI engine. SAE Tech. Pap. 2001-01-1206, 2006.

(9) Taniguchi, S.; Yoshida, K.; Tsukasaki, Y. Feasibility study of ethanol applications to a direct injection gasoline engine. SAE Tech. Pap. 2007-01-2037, 2007.

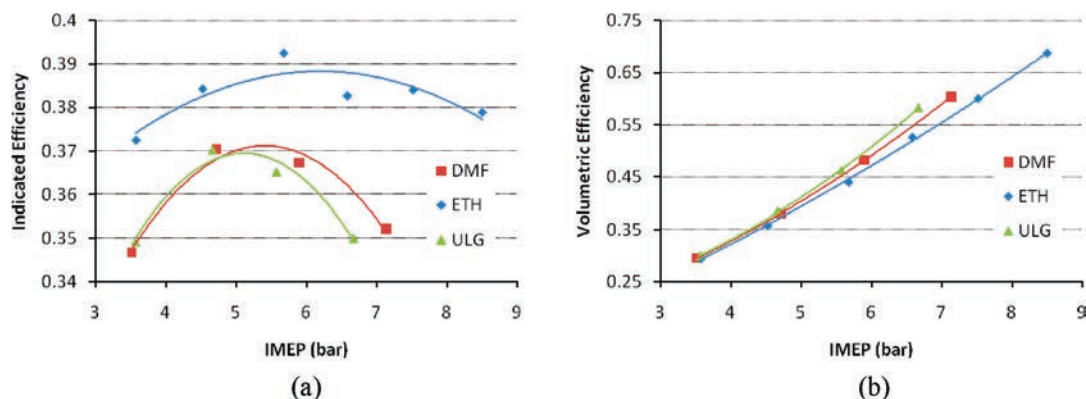


Figure 7. (a) Indicated thermal efficiency and (b) volumetric efficiency comparison for DMF, ethanol, and gasoline at 1500 rpm and $\lambda = 1.0$.

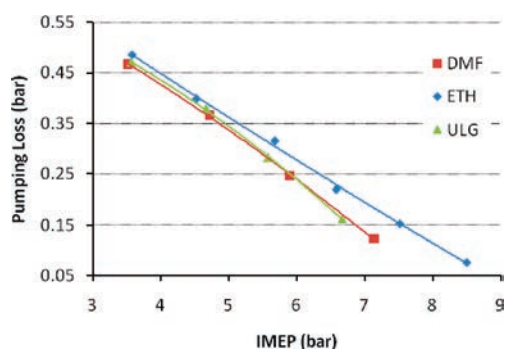


Figure 8. Pumping loss comparison for DMF, ethanol, and gasoline at 1500 rpm and $\lambda = 1.0$.

It will be shown in Figure 9 that the in-cylinder pressure and temperature are the lowest for ethanol, which increases the burn duration. It is also important to note that, for a stoichiometric air–fuel mixture, ethanol has relatively more fuel to burn, which would increase the combustion duration. The combustion duration for gasoline and DMF decreases more rapidly with respect to load. The combustion duration of DMF, however, is quicker than gasoline at 3.5 bar IMEP and marginally so around 4.5 bar IMEP. Above this load, the combustion rate of gasoline is superior. It appears that DMF has a fast flame propagation rate, which results from a rapid heat release, that has been confirmed by the currently ongoing studies on the imaging of ignition and flame development of DMF in a constant volume vessel (results will appear in a subsequent publication). DMF combustion appears to be more suited to the operating conditions optimized for gasoline. This suggests that the combustion duration of ethanol could be reduced if the engine performance parameters were optimized. This is the focus of further engine studies, and the results will follow this publication.

3.3. Thermal Efficiency. The indicated thermal efficiency of the engine is presented here because of the varying degree of oxygenation of the fuels (DMF and ethanol) used and the impact this has on the resulting gravimetric calorific value.

Figure 7a shows how the indicated efficiency of DMF is similar to gasoline. Ethanol, on the other hand, has a consistently high indicated efficiency, which is probably due to its high combustion efficiency and oxygen content (35% oxygen content by mass, 18% higher than DMF). The efficiency does not drop off as suddenly as is experienced with DMF and gasoline and remains above 37%. This advantage is partly offset by the higher pumping losses

incurred because of its lower stoichiometric air/fuel ratio. This will be discussed later (Figure 8).

The volumetric efficiency has also been used to describe the effect of the fuel properties on the engine-operating characteristics. It is defined as the volume flow rate of air into the cylinder for a given volume displacement rate of the piston. The air flow for each cycle is calculated using the measured fuel flow rate from the volumetric flow meter, and the LA4 λ meter is used to interpret the mass of fuel. Figure 7b shows that the volumetric efficiency for DMF is similar to that of gasoline and higher than ethanol. Ethanol has a lower volumetric calorific value and requires a higher quantity of fuel injection than DMF for a given engine load. In fact, the very low stoichiometric air/fuel ratio of ethanol (8.95; see Table 2) requires less air to be induced. On the other hand, the GDI engine has an advantage of mixture formation by introducing air and fuel into the cylinder independently by injection in the late induction (or compression) stroke. The high charge-cooling effect of ethanol because of its high latent heat of vaporization (see Table 2) helps to increase the air density and mass. This charge-cooling effect is evident from the lower exhaust gas temperatures seen in Figure 9b. Added to this is the throttling effect, especially for the case of ethanol, which delivers a lower quantity of air compared to DMF and gasoline. This is shown clearly in Figure 8. Here, the pumping loss is significant for ethanol, where the difference between gasoline and DMF increases with load. Higher throttling would further lower the in-cylinder temperature and combustion pressure. DMF, however, requires less throttling, which results in lower pumping losses, similar to the case of gasoline.

The corresponding maximum in-cylinder pressures and theoretically calculated maximum in-cylinder gas temperatures for the three fuels are presented in Figure 9. The in-cylinder temperature is calculated using a detailed engine gas-dynamics and thermodynamics model, where the match of experimental and simulated IMEP and maximum pressure is remarkably good. Some fundamental assumptions are made according to the book by Stone.¹⁰ Because of the higher latent heat of vaporization (see Table 2) of ethanol, which encourages a cooling effect, its in-cylinder peak gas temperature and, thus, peak pressure are much lower. It is clear that the results between DMF and gasoline are very close. DMF has a slightly lower latent heat of vaporization value and, thus, has an opposite effect on the gas temperature. The high gas temperatures for

(10) Stone, R. *Introduction to Internal Combustion Engines*, 3rd ed.; Macmillan Press, Ltd., Basingstoke, U.K., 1999; ISBN 0-333-74013-0.

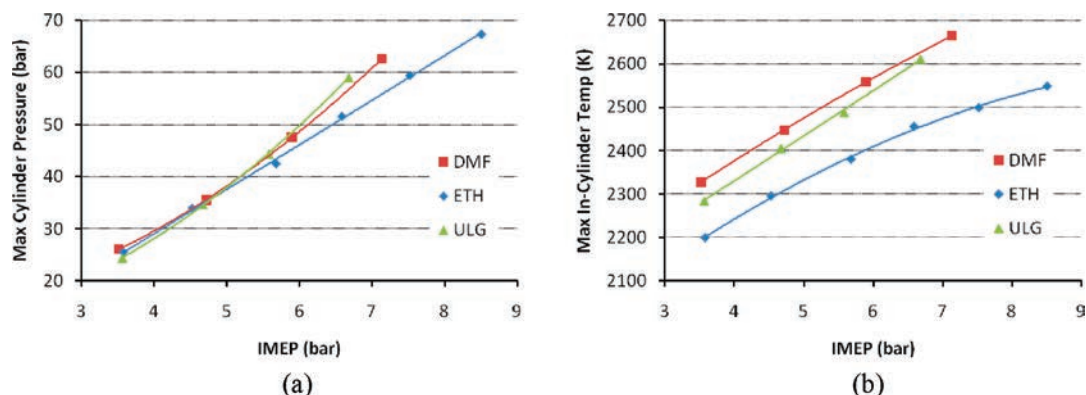


Figure 9. (a) Maximum in-cylinder pressure and (b) exhaust gas temperature under different engine loads for DMF, ethanol, and gasoline at 1500 rpm and $\lambda = 1.0$.

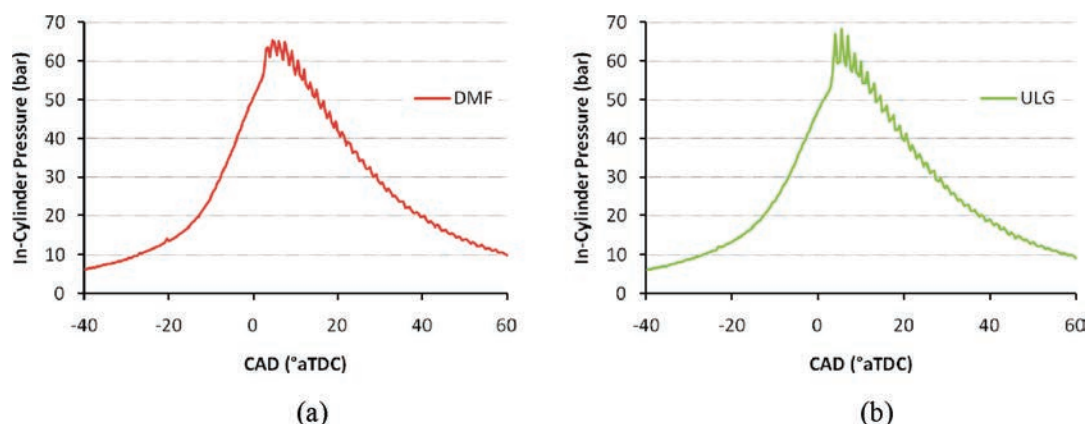


Figure 10. Raw and unfiltered pressure traces for (a) DMF at 7.1 bar and (b) gasoline at 6.7 bar, showing worst-case knock at 1500 rpm and $\lambda = 1.0$.

DMF and gasoline are expected to result in higher oxides of nitrogen (NO_x) emissions and also lead to a higher knock tendency.

3.4. Engine Knock. As previously mentioned, the constant ignition timing of 34° BTDC induced engine knock when using DMF and gasoline as the load was increased. This phenomenon was first observed at 5.5 bar. However, the authors decided to retain this load data because it affected less than 10% of the total engine cycles recorded to show the combustion characteristics of the tested fuels. The knock tendency appears to be lower with DMF than with gasoline, presumably because the former has a higher RON than gasoline. However, the severity of the knock increased with the load. Above 6.5 bar, the engine became unstable (Figure 10) and further testing would have caused severe damage. Ethanol, however, was not affected by knock at any load; therefore, the data collection was safely extended to 8.5 bar.

The COV of IMEP can be used to show the stability of combustion for the three fuels and demonstrates the consequence of knock when using DMF and gasoline. The onset of slight knock around 5.6 bar IMEP for gasoline and 5.9 bar IMEP for DMF adversely affects the engine stability. The COV of IMEP begins to increase (Figure 11), and the indicated efficiency drops (Figure 7a). This becomes much more prominent at 6.7 and 7.1 bar IMEP for gasoline and DMF, respectively. Here, the knock is more severe, which increases the COV of IMEP (especially for gasoline). Ethanol combustion, on the other hand, is relatively unaffected by the fixed timing. With increasing load, the combustion stability of ethanol actually improves slightly

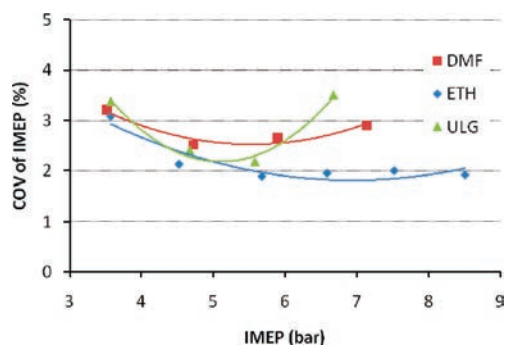


Figure 11. Covariance (COV) of IMEP for DMF, ethanol, and gasoline at 1500 rpm and $\lambda = 1.0$.

(COV of IMEP drops below 2%). Ethanol is much more resistant to knock, suggesting that it would benefit from higher compression ratios.

The purpose of this paper was to perform a preliminary comparison of DMF combustion under constant ignition timing. This, however, has introduced questions over the exact RON of the DMF fuel used in this study. Although there is little to be found on the anti-knock quality of DMF, it is thought to have a RON of 119,¹ which suggests that it is better at avoiding knock than ethanol (RON of 110). However, this was clearly not the case. Therefore, an investigation into the true knock resistance of DMF will need to be carried out.

3.5. Legislated Gaseous Emissions. Figure 12 shows the comparison of the engine-out emissions under different loads for the three fuels. In comparison to gasoline and

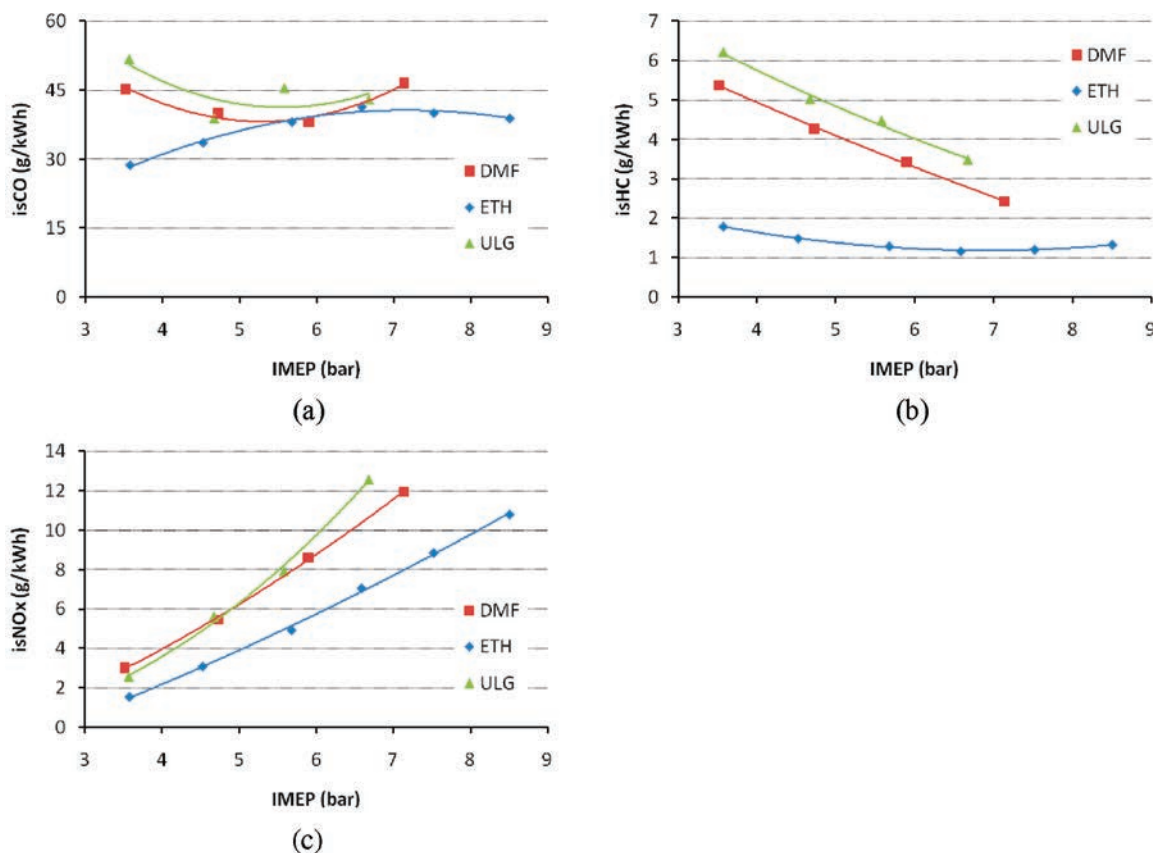


Figure 12. Indicated specific emissions: (a) CO, (b) HC, and (c) NO_x under different IMEP values for DMF, ethanol, and gasoline at 1500 rpm and $\lambda = 1.0$.

DMF, which share a similar trend and level of carbon monoxide (CO) emissions (Figure 12a), ethanol produces lower CO levels at low loads (up to 5.7 bar IMEP). It is expected that the relatively longer time required to mix the larger quantity of ethanol (because of its lower heating value) will result in a relatively poor mixture of ethanol and air. The injected fuel and inducted air in a GDI engine needs to be mixed thoroughly during a relatively short period; this is one of the main issues in the DI of gasoline and ethanol blends. Clearly, the turbulence level in the cylinder at low engine speeds (1500 rpm) and low loads was weak, and thus, the mixing process with additional ethanol was even poorer. These results have been observed by other researchers.^{11,12} Despite this drawback, ethanol produces the lowest overall emissions. Relevant evidence is being obtained through a parallel optical diagnostic study of DMF as an engine fuel. The lower CO emissions of ethanol are a result of the lower combustion temperatures (Figure 9b) and suggest that the combustion is more complete. DMF has a marginally lower indicated specific CO level compared to gasoline, which further highlights the CO emissions benefit when using oxygenated biofuels.

As shown in Figure 12b, the hydrocarbon (HC) emissions for ethanol are much lower at low engine loads compared to those for DMF and gasoline; however, the difference decreases rapidly as the engine load increases. Larger loads lead

to higher in-cylinder temperatures, which helps with the oxidation of the unburned DMF and gasoline components. The lower HC levels with ethanol could be mainly attributed to its more complete combustion and the promotion of the oxidation reaction because of the additional availability of oxygen. The level of total unburned HCs resulting from DMF combustion is between gasoline and ethanol because of the oxygen content; it also contains 16.67% oxygen by mass, as shown in Table 2.

In general, the formation of NO_x is caused by high combustion temperatures. NO_x emissions for DMF, ethanol, and gasoline are given in Figure 12c. It is clear that the NO_x emissions are load-dependent and reveal an inverse trend to total HC emissions. At the lowest load of 3.5 bar IMEP, the NO_x emission levels appear to correlate with the calculated maximum in-cylinder temperatures (Figure 9b), but at higher loads, the NO_x measurements increase rapidly when the engine approaches the knocking phenomena at 6.7 bar IMEP for gasoline (7.1 bar IMEP for DMF). The presented calculated maximum temperatures from the thermodynamic engine model give only a snapshot of the maximum quite early in the main combustion period, while the engine-out NO_x emission is also a result of the whole temperature history of the burned charge. The ethanol combustion, however, produces considerably lower NO_x emissions throughout the full-load range. The lower heat of vaporization of DMF compared to ethanol is believed to have contributed to the higher NO_x emissions. On the other hand, the lower cylinder pressures and exhaust temperatures associated with ethanol, as shown in Figure 9, have led to a significantly lower NO_x concentration.

(11) Wyszynski, L. P.; Stone, C. R.; Kalghatgi, G. T. The volumetric efficiency of direct and port injection gasoline engines with different fuels. SAE Tech. Pap. 2002-01-0839, 2002.

(12) Kapus, P. E.; Fuehrer, A.; Fuchs, H.; Fraidl, G. K. Ethanol direct injection on turbocharged SI engines—Potential and challenges. SAE Tech. Pap. 2007-01-1408, 2007.

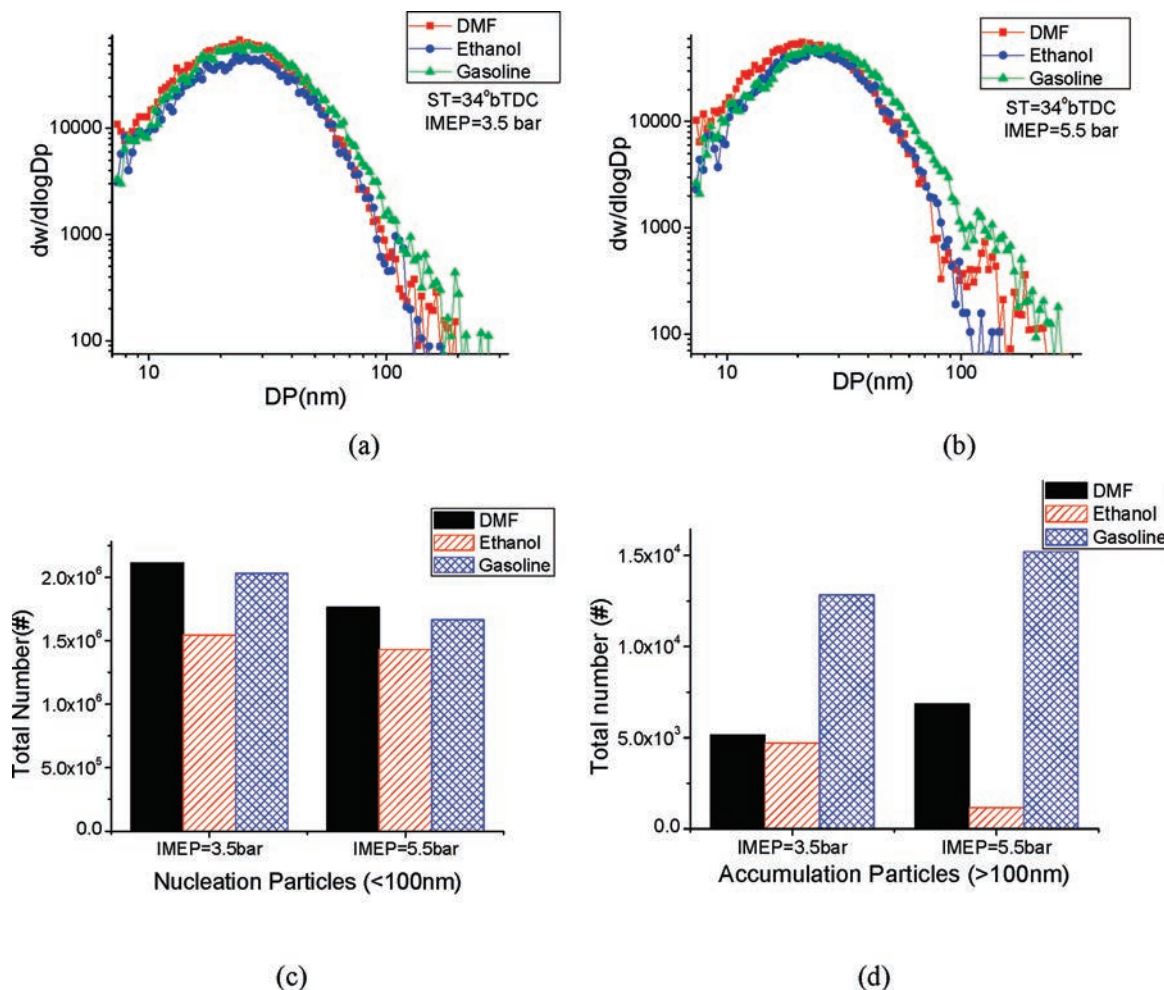


Figure 13. Particle size distributions and total numbers for DMF, ethanol, and gasoline at 1500 rpm and $\lambda = 1.0$.

3.6. PM Emissions. Figure 13 presents the number-based particulate size distribution in the exhaust gas for the three fuels. Figure 13a clearly shows that particulates for DMF, ethanol, and gasoline at 3.5 bar IMEP have a similar distribution and most of them are in the nucleation mode and peak around 20–30 nm. Increasing the IMEP has some impact on the particle size distributions. When the IMEP is increased from 3.5 to 5.5 bar IMEP, as shown in Figure 13b, the number of nucleation mode particles was reduced by 10–15% and more accumulation mode particles were produced. This effect was more significant when the engine was fueled with DMF and gasoline, because the diameter of the nucleation mode particle peak tended to become smaller (Figure 13c) and a clear peak formed in the number of accumulation mode particles. The gasoline combustion, however, produced the highest number of total accumulation particles of the three fuels. Figure 13d highlights this significance. At 3.5 bar, the total accumulation particles for gasoline are much higher than for DMF and ethanol. This gap becomes more significant at 5.5 bar, where the total number of particles exceeds 15 000, which is almost double the number of particles produced by DMF and 14 000 more than ethanol.

Figure 14a shows the total particle concentration emitted when using the three fuels. In comparison to the other two fuels, fueling with ethanol results in the lowest PM emissions for both engine conditions (3.5 and 5.5 bar IMEP), while DMF produced slightly more particles than gasoline by 2000 particles/cm³. The increase of IMEP led to

the reduction of particle numbers by around 5500 particles/cm³ from 33 200 to 27 700 particles/cm³ for DMF, by 1800 particles/cm³ from 24 200 to 22 400 particles/cm³ for ethanol and by 5700 particles/cm³ from 31 950 to 26 250 particles/cm³ for gasoline. This was probably due to the increased combustion temperature with higher load, which leads to more pyrolysis, which is also reflected in Figure 13. Here, more accumulation mode particles were produced at higher loads, which was especially significant for both DMF and gasoline.

According to Figure 14b, the mean diameter of the particles emitted when fueled with gasoline was the largest of the three, while the mean diameter of those produced by DMF was the smallest. The increase of IMEP not only lowered the particle number concentration for all of the fuels (at the cost of some increase in accumulation mode particles) but also reduced the particle mean diameter of DMF and ethanol. However, this did not affect the mean diameter of particles emitted with gasoline fueling. This is likely to be related to the difference in the number of fuel droplets in the injection process, where DMF has a lower viscosity and breakup surface tension, which leads to smaller sized fuel particles. These issues are currently under study.

4. Conclusions

Comparative engine tests with DMF, ethanol, and gasoline were performed to understand the potential of DMF as a novel biofuel, as well as the performance issues and emissions

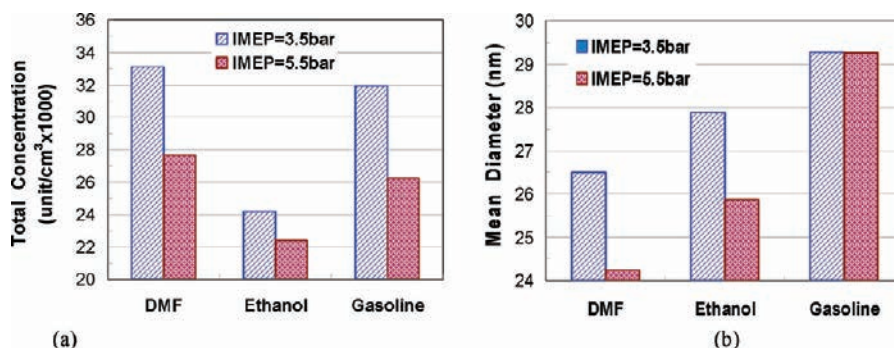


Figure 14. (a) Particle concentrations and (b) count-averaged mean diameter for DMF, ethanol, and gasoline at 1500 rpm and $\lambda = 1.0$.

associated with its use. The single-cylinder engine was tested using a constant spark timing of 34° BTDC between 3.5 and 8.5 bar. The following conclusions can be made: (1) Similar to ethanol, DMF can be a viable biofuel, assuming that adequate availability and sustainability will not be an issue. Using pure DMF as a fuel on a research engine did not show any apparent adverse effects on the engine for the duration of the experiments. (2) The initial combustion duration of DMF is shown to be shorter than that of gasoline. When it is compared to ethanol, the difference varies with load, so that it is longer at low-load conditions but shorter at higher load conditions. (3) The constant ignition timing of 34° BTDC induced severe engine knock for DMF at 7.1 bar IMEP and gasoline at 6.5 bar IMEP. (4) Ethanol showed no signs of knock, and the load could be extended safely to 8.5 bar IMEP. The onset of knock for DMF at loads similar to gasoline was somewhat unexpected. This justifies a further study into the real octane number for DMF, which is given in early studies as higher than that of ethanol. (5) The emissions of CO, HC, and NO_x using DMF are all similar to those with gasoline. Ethanol combustion produces lower CO emissions because of the lower maximum in-cylinder temperature and possibly more complete combustion. At lower loads, ethanol produces lower HCs, probably because of its relatively high oxygen content, which gives rise to more complete combustion. Ethanol also produces lower NO_x emissions for the whole load range, possibly because of its higher latent heat of evaporation, which leads to a relatively lower in-cylinder temperature. (6) PM emissions of DMF are similar to that of gasoline. DMF actually produced the smallest mean diameter sized particles of the three fuels and a similar concentration to gasoline, which suggests the total mass of PM for DMF is the lowest. (7) Overall, the experiments confirm that, because of the similar physicochemical properties of DMF and gasoline, DMF exhibits very similar combustion and emissions characteristics to gasoline. This indicates that DMF may be suitable to use as an existing gasoline-type engine fuel and that no major modifications and adjustments would be needed to produce an equivalent engine performance and emissions level.

To supplement this investigation, detailed engine testing using the MBT timings for the three fuels is being carried out and will follow this report. Modeling and optical studies of the spray behavior and chemical kinetics of the oxidation reactions of DMF are ongoing and will explore, in more detail, the in-cylinder combustion initiation and development. In addition, a critical issue for biofuels and automotive fuels in general is the presence

of any toxic components in the engine-out emissions. Therefore, further tests concerning the speciation of emissions for DMF are underway.

Acknowledgment. This work was conducted in the Future Engines and Fuels Lab at the University of Birmingham and financially supported by the Engineering and Physical Sciences Research Council (EPSRC) through the Research Grant EP/F061692/1. The authors thank Professor Frank Palmer for his contributive discussions and Jaguar Cars and Shell Global Solutions U.K. for their generous support and contribution. The authors thank Peter Thornton and Carl Hingley for their technical support of the engine testing facility and Farshad Eslami for his contribution to the measurement of the calorific values of the tested fuels. The authors also acknowledge their international collaborators Tsinghua University and Wuhan University of Technology for their support.

Note Added after ASAP Publication. Figure 4 and the first two paragraphs in the Results and Discussion section were modified in the version of this paper published ASAP April 9, 2010; the corrected version published ASAP April 15, 2010.

Nomenclature

ATDC = after top dead center
 BTDC = before top dead center
 CAD = crank angle degree
 CO = carbon monoxide
 COV = coefficient of variation
 CPC = condensation particle counter
 DI = direct injection
 DMA = differential mobility analyzer
 DMF = 2,5-dimethylfuran
 EGR = exhaust gas recirculation
 EVC = exhaust valve closing
 HC = hydrocarbon
 IMEP = indicated mean effective pressure
 IVO = intake valve opening
 LCV = lower calorific value
 MFB = mass fraction burned
 NO_x = oxides of nitrogen
 PM = particulate matter
 RON = research octane number
 rpm = revolutions per minute
 SMPS = scanning mobility particle sizer
 SOI = start of injection
 TDC = top dead center
 λ = excess air ratio